Million-Q Reflection-Based Integrated Resonators Patterned With Deep Ultraviolet Photolithography

Christoph M. Greiner, *Member, IEEE*, Dmitri Iazikov, *Member, IEEE*, and Thomas W. Mossberg, *Member, IEEE*

***Abstract*—We describe million-Q one- and two-dimensional integrated reflective resonators based on ultralow-loss etched Bragg reflectors patterned on silica-on-silicon slab and channel waveguides using deep ultraviolet photoreduction lithography. Measured device performance, obtained in the limit of high reflectivity, provides insights in loss mechanisms operative in the subject systems. Implementation of integrated reflection-based resonators with high-Q and finesse values promises new directions in photonic integration with applications in sensing, filtering, and signal transport.**

***Index Terms*—Etched Bragg gratings, holographic Bragg reflector (HBR), integrated resonator, planar lightwave circuit, silica-on-silicon waveguides.**

I. Introduction

MANY critical signal processing functions including modulation and filtering depend on or can be enhanced using optical resonators. In the domain of integrated photonics, resonators have been largely based on recirculating guided-wave structures such as channel waveguide rings, which can be evanescently coupled to adjacent linear channel waveguides. The low losses achievable in channel waveguides, especially in the silica-on-silicon format, have yielded ring resonators with finesse values in excess of 100 and quality factors larger than ten million [1]. Much less work has been reported on integrated resonators based on reflective optics [2]–[5].

Recent advances in deep ultraviolet (DUV) reduction photolithographic patterning tools have enabled the scribing of essentially arbitrary diffractive structures with feature sizes even below 100 nm. Recognition of the powerful potential inherent to DUV photolithography for integrated photonics fabrication is presently emerging in the community [6]–[9]. Here, we use DUV photolithography to create reflective resonators employing distributed Bragg mirrors with straight and curved diffractive contours in channel and slab resonators, respectively, and demonstrate resonator quality factors in excess of one million. To achieve high quality factors in a single-mode channel waveguide, only high reflectivity and low loss are required (as in a fiber-based resonator). In a slab resonator, the Q-factor is additionally affected by wavefront deformation arising from mirror surface irregularities and slab waveguide nonuniformities, such as index inhomogeneities and thickness variation. The present results are surprising in that they demonstrate extraordinarily high fidelity in the DUV photolithographic patterning process (providing for curved mirrors of extreme figure precision) and they demonstrate the very high effective refractive-index uniformity that can be achieved in silica-on-silicon slab waveguide structures. Distributed mirrors fashioned via DUV photolithography have the added advantage of being compatible with advanced apodization methods [6], [7], providing precise control over their overall spectral transfer function. Tailoring of the mirror passbands allows one to critically influence the overall resonator spectral response. We note that reflective resonators have been implemented in fibers via fiber Bragg gratings—a useful but nonintegrated format.

We have reported on a two-dimensional (2-D) integrated reflective resonator [2] in the past. Our previous results were obtained in the extremely overcoupled regime, where resonator behavior was dominated by the high ($\sim$30%) transmission loss of the low-reflectivity mirrors rather than other fabrication or material-related loss mechanisms. Accordingly, no information about format-limiting performance could be obtained. Here, we report on resonator behavior in the undercoupled (low mirror transmission) regime, allowing for the first time for straightforward experimental evaluation of the resonator's *inherent* finesse and quality factor which are found to be larger by more than an order of magnitude than previously reported results.

II. Results

A. High-Q Slab Waveguide Resonator

A schematic top view of the 2-D slab-waveguide-based resonator is shown in Fig. 1(a). Two 600-μm-long curved holographic Bragg reflectors (HBRs) function as mirrors in this asymmetric concave/convex concentric resonator design. HBR mirrors are spaced by 4 mm, yielding a design free spectral range (FSR) of $\sim$26 GHz, and have circular lines concentric about point "C" (located at the endpoint of the resonator's input channel waveguide to the left of the cavity) with radii of 3 and 7 mm. The signal emerges from the channel waveguide, expands in the open slab region at the left hand and subsequently, if resonant, builds up in the resonator. The input channel waveguide has an opening of about 13 μm, adiabatically increased from about 4 μm at the die edge via a 0.5-mm-long taper.

A partial cross-sectional view of one of the resonator's HBR mirrors is given in Fig. 1(b). In the HBR region, the silica slab waveguide consists of a doped dual-layer core and bilateral 15-μm-thick cladding layers. The dual-layer core comprises a 500-nm-thick grating layer which has a +3% refractive index contrast relative to the cladding and $\sim$2-nm-thick upper core layer with a +1% refractive contrast relative to the cladding. Depicted at the interface between the two core sublayers are

Manuscript received August 30, 2006; revised October 11, 2006.

The authors are with LightSmyth Technologies Inc., Eugene, OR 97401 USA (e-mail: cgreiner@lightsmyth.com).

Digital Object Identifier 10.1109/LPT.2006.887885

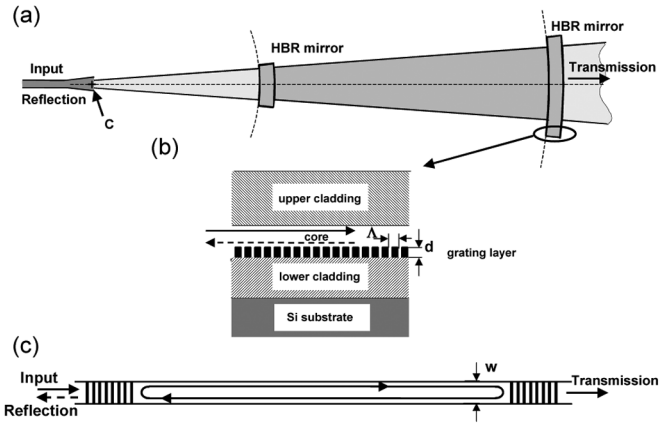

Fig. 1. Schematic of integrated cavities. (a) Top view showing 2-D cavity comprising two HBRs functioning as resonator mirrors and input channel waveguide. HBR mirrors are concentric about center of curvature C. (b) Cross-sectional view of grating section for 1-D and 2-D cavities d grating height; Λ, grating period. (c) Top view of channel waveguide resonator w waveguide width.

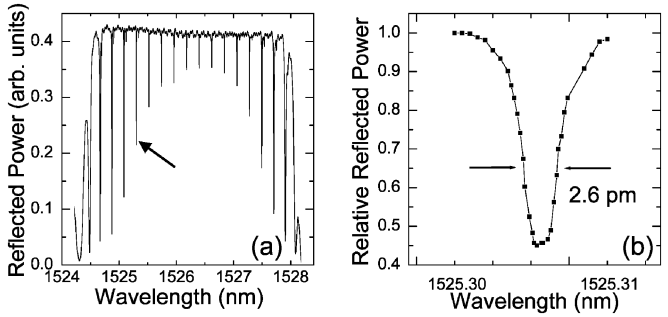

Fig. 2. (a) Resonator reflection profile of 2-D integrated resonator. (b) Blow-up of individual resonator transmission mode. All data shown were measured with TM polarization.

cross sections of representative lithographically patterned grating contours. The diffractive contours consist of trenches etched into the grating layer and filled with material of the upper core sublayer. The HBR mirror operates in first diffractive order with a contour spacing Λ of about 500 nm, i.e., one half of the in-medium wavelength of resonant light. Outside the grating region, the core is a single layer of the same material as the upper core with a thickness of 2.3 μm.

The Bragg structures comprising the resonators were realized in the lower subcore employing a DUV optical scanner with 4 $\times$ reduction ratio from a laser-written chromium-on-quartz reticle and subsequent reactive ion etching. Following the chemical vapor deposition of the upper core layer, the channel waveguides were defined via i-line photolithography and etch followed by final cladding deposition.

Fig. 2(a) shows the resonator's reflection spectrum as measured with TM-polarized input light. Periodic dips in the spectrum correspond to the resonator modes. The overall envelope of the $\sim$3.5-nm-wide reflection spectrum is set by the passband of the individual HBR end mirrors. Fig. 2(b) is a blow up of one of the resonator modes. The location of this resonator mode within the overall spectrum is indicated by the arrow in Fig. 2(a). As can be seen in Fig. 2(a), modes closer to the endmirror band center were damped by excess reflectivity. As can be seen in Fig. 2(b), the full-width at half-maximum of the chosen resonator mode is $\sim$2.6 pm (335 MHz). The resonator's measured FSR of $\sim$220 pm (28 GHz) yields a finesse of 84. The quality factor of the resonator is almost one million, specifically 6×10^5. From the measured finesse value and contrast between on- and off-resonant reflected power, the reflectivity of an individual HBR mirror and the single-pass resonator loss (at the wavelength of the mode characterized) are estimated to be 98.9% and 2.7%, respectively. The total insertion loss of the resonator (in reflection) was found to be 2.0 dB, of which 1.5 dB result from fiber-to-waveguide coupling. For TE input, the resonator spectrum is red-shifted by 40 pm. A slightly higher mirror reflectivity (99.4%) and resonator loss (3.1%) are observed, while other parameters, within measurement accuracy, match the results for TM input.

In a 2-D resonator like that shown in Fig. 1(a), imperfections in the slab waveguide (thickness or refractive index inhomogeneity) or surface figure of HBR lines introduce wavefront errors that limit finesse by acting as a modal loss mechanism [2]. In free-space resonators, analogous wavefront distortions lead to so-called flatness finesse limits. The present finesse result indicates that the total optical wavefront error introduced by the combined influence of surface figure errors and waveguide index nonuniformity in a single pass is better than $\lambda/150$ (i.e., about 10 nm). One can deduce that the mirror surface flatness and waveguide index homogeneity are better than about $\lambda/150$ and a few 10^{-6}, respectively. These values are reminiscent of those of a free-space resonator yet exist in a fully integrated format.

Our present measurement, obtained in the undercoupled resonator regime, where behavior is dominated by format (waveguide and mirror figure imperfections) rather than mirror-transmission-based loss (as in previous work [2]), allows to accurately evaluate the available inherent quality factor Q_0 and finesse F_0 (in the limit of no mirror transmission loss) ultimately obtainable in the present implementation. By using measured resonator loss and setting the mirror reflectivity to unity, we find $Q_0 \approx 10^6$ and $F_0 \approx 120$.

B. High-Q Channel Waveguide Resonator

Fig. 1(c) is a schematic top view of a second integrated resonator based on a one-dimensional (1-D) channel waveguide. Two 500-μm-long, DUV-lithographically patterned, straight-line Bragg reflectors are located within a channel waveguide of width $w = 5$ μm. Each mirror has a $\sim$3.3-nm-wide reflection band centered at about 1522.6 nm. A 3-cm mirror spacing was chosen to maximize the relative importance of propagation loss as consistent with available desing length set by the 33-mm-long optical stepper exposure field. The cavity FSR is about 3.4 GHz. Resonant light enters the resonator through the left mirror shown in Fig. 1(c). Grating parameters and waveguide layer dimensions are identical to those shown in Fig. 1(b).

Fig. 3 shows part of the resonator transmission spectrum slightly to the blue of the mirror reflection band center, measured using a TE-polarized tunable narrow-linewidth laser. The

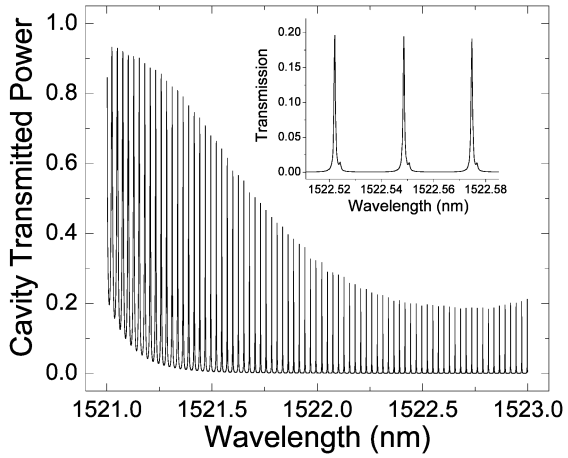

Fig. 3. Partial resonator transmission profile. Periodic peaks in the measured transmission spectrum correspond to resonant resonator modes. The inset to the main graph shows a spectrum blow-up near the band center. All data shown were measured with TE polarization.

periodic peaks observed correspond to the resonator modes. The inset to Fig. 3 shows several transmission peaks on an expanded horizontal scale. The transmitted power shown in Fig. 3 is normalized relative to far red-detuned laser transmission. Fiber-to-waveguide coupling loss at all signal wavelengths was 1.45 dB. From Fig. 3, the resonator's FSR and bandpass were determined to be 3.4 ($\pm$0.04) GHz and 88 (10) MHz, respectively. The FSR observed is consistent with the 3-cm mirror separation. The resonator finesse is 38.6 (4.8). The quality factor of the integrated channel resonator was found to be 2.24 (0.25) $\times 10^6$. The resonator's inherent quality factor and finesse are extrapolated to be $Q_0 = 4 \times 10^6$ and $F_0 \approx 70$. The measured FSR and finesse are independent of polarization to within measurement uncertainty. Mirror reflection passbands for TE polarization are red-shifted by 170 pm relative to those observed with TM. The origin of polarization-dependent shifts in channel and slab resonators is believed to be stress-induced birefringence [2], [10].

From the measured resonator transmission of 19.3 (0.2)%, shown in the inset to Fig. 3, and the finesse value above, we estimate the single-pass internal loss to be 4.5% (0.5%) and the mirror reflectivity to be about 96.5%. It is interesting to note that the channel waveguide resonator loss per unit length is about five times smaller than that of the 2-D resonator. This result may indicate that surface figure and/or index inhomogeneity, which is important primarily in the case of the 2-D resonator, does play the ultimate role in limiting its performance.

III. Conclusion

One-dimensional and two-dimensional integrated waveguide resonators based on photolithographically patterned and etched Bragg reflectors have been shown to achieve quality factors of several millions, an improvement by more than an order of magnitude over previous work [2], providing for the first time insight into the ultimately obtainable performance. Quality factors and finesse values are close to the best values in a silica-on-silicon based ring resonator [1] but have footprints smaller by more than three (two) orders of magnitude than the latter for the channel (slab) resonator. Folded reflective cavities allow access to FSRs larger than obtainable in low-index-contrast (of a few percent) rings which are ultimately constrained by bending loss considerations [2]. An advantage of the physically distinct grating end mirrors is that their spectral response can be controlled by apodization and/or chirping—a task that becomes straightforward using the DUV photolithographic patterning approach—thus allowing one to control the overall resonator passbands and spectral behavior. Stamping-based production [10] from photolithographically fabricated masters provides a pathway to high-volume low-cost devices that may find application in sensing. Here, an HBR resonator with an exposed evanescent intracavity field uniquely provides a fully 2-D sampling surface. Wafer-bonding an electrooptic or gain material onto the exposed evanescent intracavity field may enable efficient hybrid integrated modulators and lasers [11].

References

[1] R. Adar, M. R. Serbin, and V. Mizrah, "Less than 1 dB per meter propagation loss of silica waveguides measured using a ring resonator," *J. Lightw. Technol.*, vol. 12, no. 8, pp. 1369–1369, Aug. 1994.

[2] C. M. Greiner, D. Iazikov, and T. W. Mossberg, "Low loss silica-on-silicon two-dimensional Fabry–Perot cavity based on holographic Bragg reflectors," *Opt. Lett.*, vol. 30, pp. 38–38, 2005.

[3] T. F. Krauss, B. Vogele, C. R. Stanley, and R. M. De La Rue, "Waveguide microcavity based on photonic microstructures," *IEEE Photon. Technol. Lett.*, vol. 9, no. 2, pp. 176–176, Feb. 1997.

[4] H. K. Tsang, M. W. K. Mak, L. Y. Chan, J. B. D. Soole, C. Youtsey, and I. Adesida, "Etched cavity InGaAsP–InP waveguide Fabry–Perot filter tunable by current injection," *J. Lightw. Technol.*, vol. 17, no. 10, pp. 1890–1890, Oct. 1999.

[5] C. A. Barrios, V. R. Almeida, R. R. Panepucci, B. S. Schmidt, and M. Lipson, "Compact silicon tunable Fabry–Pérot resonator with low power consumption," *IEEE Photon. Technol. Lett.*, vol. 16, no. 2, pp. 506–506, Feb. 2004.

[6] T. W. Mossberg, C. Greiner, and D. Iazikov, "Interferometric amplitude apodization of integrated gratings," *Opt. Express*, vol. 13, pp. 2419–2419, 2005.

[7] C. Greiner, D. Iazikov, and T. W. Mossberg, "Lithographically fabricated planar holographic Bragg reflectors," *J. Lightw. Technol.*, vol. 22, no. 1, pp. 136–145, Jan. 2004.

[8] W. Bogaerts, V. Wiaux, D. Taillaert, S. Beckx, B. Luyssaert, P. Bienstmann, and R. Baets, "Fabrication of photonic crystals in silicon-on-insulator using 248-nm deep UV photolithography," *J. Sel. Topics Quantum Electron.*, vol. 8, no. 4, pp. 928–928, Jul./Aug. 2002.

[9] M. Settle, M. Salib, A. Michaeli, and T. F. Krauss, "Low loss silicon on insulator photonic crystal waveguides made by 193 nm optical lithography," *Opt. Express*, vol. 14, pp. 2440–2440, 2006.

[10] J. Liu, Y.-L. Lam, Y.-C. Chan, Y. Zhou, B. S. Ooi, G. Tan, and J. Yao, "Embossed Bragg gratings based on organically modified silane waveguides in InP," *Appl. Opt.*, vol. 39, no. 27, pp. 4942–4945, 2000.

[11] A. W. Fang, H. Park, O. Cohen, R. Jones, M. J. Paniccia, and J. E. Bowers, "Electrically pumped hybrid AlGaInAs-silicon evanescent laser," *Opt. Express*, vol. 14, no. 20, pp. 9203–9210, 2006.